

Article

Lecanicilliums A–F, Thiodiketopiperazine-Class Alkaloids from a Mangrove Sediment-Derived Fungus *Lecanicillium kalimantanense*

Lin-Fang Zhong^{1,2}, Juan Ling¹, Lian-Xiang Luo³ , Chang-Nian Yang³ , Xiao Liang¹ and Shu-Hua Qi^{1,*}

¹ CAS Key Laboratory of Tropical Marine Bio-Resources and Ecology, Guangdong Key Laboratory of Marine Materia Medica, South China Sea Institute of Oceanology, Chinese Academy of Sciences, Guangzhou 510301, China; 18851107875@163.com (L.-F.Z.); lingjuan@scsio.ac.cn (J.L.); liangxiao@scsio.ac.cn (X.L.)

² University of Chinese Academy of Sciences, Beijing 100049, China

³ The Marine Biomedical Research Institute, Guangdong Medical University, Zhanjiang 524023, China; luolianxiang321@gdmu.edu.cn (L.-X.L.); nicholasyeung@gdmu.edu.cn (C.-N.Y.)

* Correspondence: shuhuaqi@scsio.ac.cn; Tel.: +86-208-9022-112; Fax: +86-208-4458-964

Abstract: Six new thiodiketopiperazine-class alkaloids lecanicilliums A–F were isolated from the mangrove sediment-derived fungus *Lecanicillium kalimantanense* SCSIO41702, together with thirteen known analogues. Their structures were determined by spectroscopic analysis. The absolute configurations were determined by quantum chemical calculations. Electronic circular dichroism (ECD) spectra and the structure of Lecanicillium C were further confirmed by a single-crystal X-ray diffraction analysis. Lecanicillium A contained an unprecedented 6/5/6/5/7/6 cyclic system with a spirocyclic center at C-2'. Biologically, lecanicillium E, emethacin B, and versicolor A displayed significant cytotoxicity against human lung adenocarcinoma cell line H1975, with IC₅₀ values of 7.2–16.9 μM, and lecanicillium E also showed antibacterial activity against four pathogens with MIC values of 10–40 μg/mL. Their structure–activity relationship is also discussed.

Keywords: mangrove sediment-derived fungus; *Lecanicillium kalimantanense*; thiodiketopiperazine-class alkaloid; cytotoxicity; antibacterial



Citation: Zhong, L.-F.; Ling, J.; Luo, L.-X.; Yang, C.-N.; Liang, X.; Qi, S.-H. Lecanicilliums A–F,

Thiodiketopiperazine-Class Alkaloids from a Mangrove Sediment-Derived Fungus

Lecanicillium kalimantanense. *Mar. Drugs* **2023**, *21*, 575. <https://doi.org/10.3390/md21110575>

Academic Editor: Jie Bao

Received: 2 October 2023

Revised: 21 October 2023

Accepted: 24 October 2023

Published: 31 October 2023



Copyright: © 2023 by the authors. Licensee MDPI, Basel, Switzerland. This article is an open access article distributed under the terms and conditions of the Creative Commons Attribution (CC BY) license (<https://creativecommons.org/licenses/by/4.0/>).

1. Introduction

Natural products containing sulfur exhibit significant structural diversities and diverse biological activities [1,2]. Among them, thiodiketopiperazine, as an interesting subgroup, is an important class of secondary metabolites of fungi, especially species of *Aspergillus fumigatus*, *A. terreus*, *A. flavus*, *A. niger*, *Trichoderma virens*, *T. viride*, and *Penicillium terlikowskii* [3]. The structures of thiodiketopiperazines are diverse [4,5], of which the spirocyclic thiodiketopiperazines are rare in nature [5,6]. Many thiodiketopiperazines have been reported to display a wide range of biological properties, including antiproliferative, cytotoxic, antibacterial, antifungal, antiviral, and anti-angiogenic activities [7,8]. For examples, brocazine G displayed potent antibacterial activity against *Staphylococcus aureus* with a MIC value of 0.25 μg/mL and strong cytotoxicity against human ovarian cancer cells (IC₅₀ = 0.66 μM) [8]. Penicisulfuranols A–C showed cytotoxicity towards human cervical carcinoma cell lines and human promyelocytic leukemia cells with IC₅₀ values of 0.1–3.9 μM [9]. Penicibrocazine C exhibited antibacterial activity against *Micrococcus luteus* with MIC value of 0.25 μg/mL, which was stronger than the positive control, chloromycetin (MIC = 2.0 μg/mL) [10]. Numerous structurally unique and potential variety activities of the thiodiketopiperazines have drawn much attention from synthetic chemists and pharmacologists.

The fungal genus *Lecanicillium* (formerly *Verticillium*), including *L. fusisporum*, *L. psalliotae*, and *L. lecanii*, are pathogenic fungi that are widely used as biological pesticides [11–13]. The secondary metabolisms of these fungi are rarely reported [11]. Only a few compounds

belonging to indolosesquiterpenoids, phenopicolinic acid derivatives, tetracyclic diterpenoids, pregnanes, and cyclic lipodepsipeptides have been isolated from the genus *Lecanicillium* up to now [14–16]. The fungus *L. kalimantanense* SCSIO41702 was isolated from a mangrove sediment sample collected from Hainan province. There was no report about the secondary metabolisms of *L. kalimantanense*. In order to explore novel, natural compounds from fungi, we investigated the secondary metabolisms of *L. kalimantanense* SCSIO41702, which led to the isolation of six new thiodiketopiperazine-class alkaloids, lecanicilliums A–F (1–6), together with thirteen known analogues (Figure 1): emethacin B (7) [17], bisdethiobis(methylsulfanyl)acetylaranotin (8) [8], bisdethiobis(methylsulfanyl)deacetylaranotin (9) [8], bisdethiobis(methylsulfanyl)aranotin (10) [8], 8-acetyl-bisdethiobis(methylsulfanyl)apoaranotin (11) [18], bisdethiobis(methylsulfanyl)acetylapoaranotin (12) [8], bisdethiobis(methylsulfanyl)apoaranotin (13) [19], bisdethiobis(methylsulfanyl)deacetylapoaranotin (14) [8], haematocin (15) [8], versicolor A (16) [20], 12,12a-anhydro-desacetyl-bis-dethio-7a, 14a-di-(methylmercapto)-apoaranotin (17) [21], emestrin H (18) [22], and citriperazine B (19) [23]. These compounds were evaluated for their cytotoxicity, toxicity against brine shrimps, and antibacterial activity. Herein, we report the isolation and structural elucidation as well as the biological activities of these compounds.

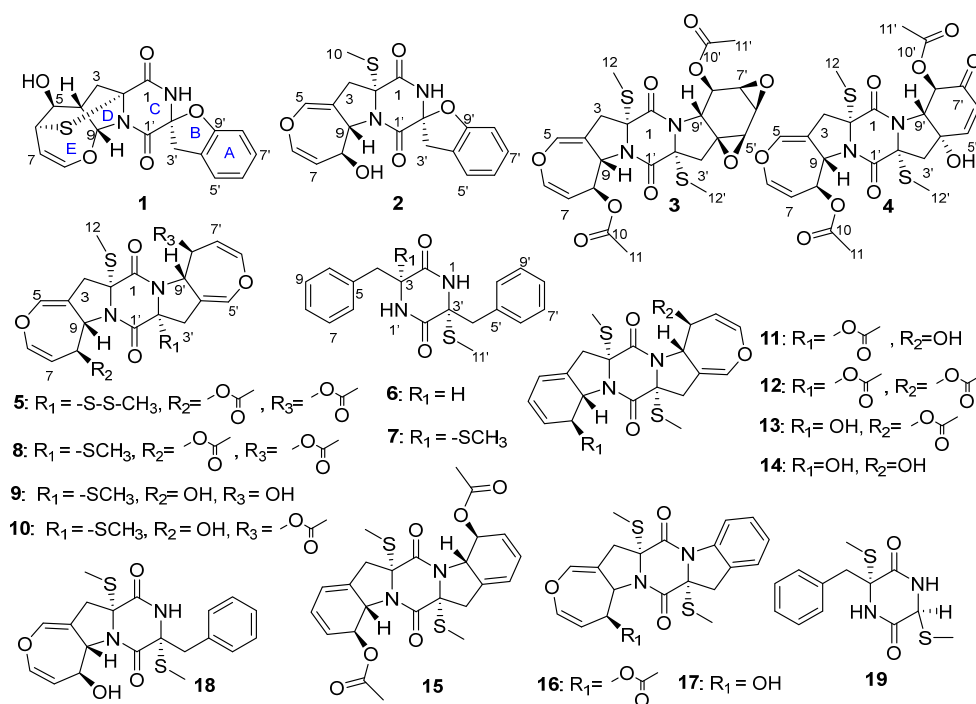


Figure 1. Structures of compounds 1–19 isolated from *L. kalimantanense* SCSIO41702.

2. Results and Discussion

Lecanicillium A (1) was obtained as a white powder with the molecular formula $C_{18}H_{16}N_2O_5S$ as determined by HRESIMS ($[M + H]^+$ m/z 373.0851) and NMR data. The 1H NMR spectrum (Table 1) displayed the presence of two active hydrogens at δ_H 10.06 (1H , s), 5.31 (1H , s), four aromatic hydrogens at δ_H 7.26 (1H , d, $J = 7.5$ Hz), 7.14 (1H , t, $J = 8.0$ Hz), 6.92 (1H , t, $J = 7.5$ Hz), 6.81 (1H , d, $J = 8.0$ Hz), two olefinic methines at δ_H 6.00 (1H , d, $J = 6.5$ Hz), 4.82 (1H , ddd, $J = 7.8, 6.5, 1.2$ Hz), four tertiary methine groups at δ_H 6.61 (1H , d, $J = 6.5$ Hz), 4.86 (1H , ddd, $J = 7.8, 6.5, 1.2$ Hz), 3.87 (1H , d, $J = 6.5$ Hz), 3.06 (1H , t, $J = 6.5$ Hz), and two methylenes at δ_H 3.94 (1H , d, $J = 16.4$ Hz), 3.26 (1H , d, $J = 16.4$ Hz), 2.71 (1H , dd, $J = 12.7, 6.5$ Hz), 2.21 (1H , d, $J = 12.7$ Hz). The ^{13}C NMR spectrum (Table 2) displayed 18 carbon signals including two methylenes, ten methines (six aromatic/olefinic and three oxygenated or heteroatomic), and six nonprotonated carbons (two diagnostic amide carbonyl, two olefinic and two heteroatomic). These NMR data of 1 (Tables 1 and 2) showed similarity to those of spirobrocazines A–C [5], which suggested

that **1** was a thiodiketopiperazine alkaloid. Detailed analysis of HSQC, HMBC and COSY spectra (Figure 2) proved that **1** contained the same structural parts of rings A–C as those of spirobrocazines A–C. However, the COSY spectrum (Figure 2) showing correlations from H-4 (δ_{H} 3.06, ^1H , t, $J = 6.5$ Hz) to H_b-3 [δ_{H} 2.71 (^1H , dd, $J = 12.7, 6.5$ Hz)], H-5 (δ_{H} 3.87, ^1H , d, $J = 6.5$ Hz) and H-9 (δ_{H} 6.61, ^1H , d, $J = 6.5$ Hz), from H-5 to H-6 (δ_{H} 4.86, ^1H , ddd, $J = 7.8, 6.5, 1.2$ Hz), and from H-7 (δ_{H} 4.82, ^1H , ddd, $J = 7.8, 6.5, 1.2$ Hz) to H-6 and H-8 (δ_{H} 6.00, ^1H , d, $J = 6.5$ Hz), and the HMBC spectrum (Figure 2) showing correlations from H-4 to C-2 (δ_{C} 70.8), C-3 (δ_{C} 48.2), C-6 (δ_{C} 52.5), from OH-5 to C-5 (δ_{C} 69.9), from H-6 to C-2, C-4 (δ_{C} 46.3), C-5, C-7, C-8 (δ_{C} 144.9), from H-8 (δ_{H} 6.00, ^1H , d, $J = 6.5$ Hz) to C-6, C-7 (δ_{C} 100.6), C-9 (δ_{C} 92.9), from H-9 to C-2, C-5, C-8, and from H-3 to C-2, C-4, C-9, suggested the presence and assignment of D/E rings in **1** as shown. Combining the molecular formula and the chemical shifts of C-2 and C-6/H-6, it was reasonable to infer a sulfide bond between C-2 and C-6 to form a sulfide six-membered-ring. Thus, the planar structure of **1** was determined as shown.

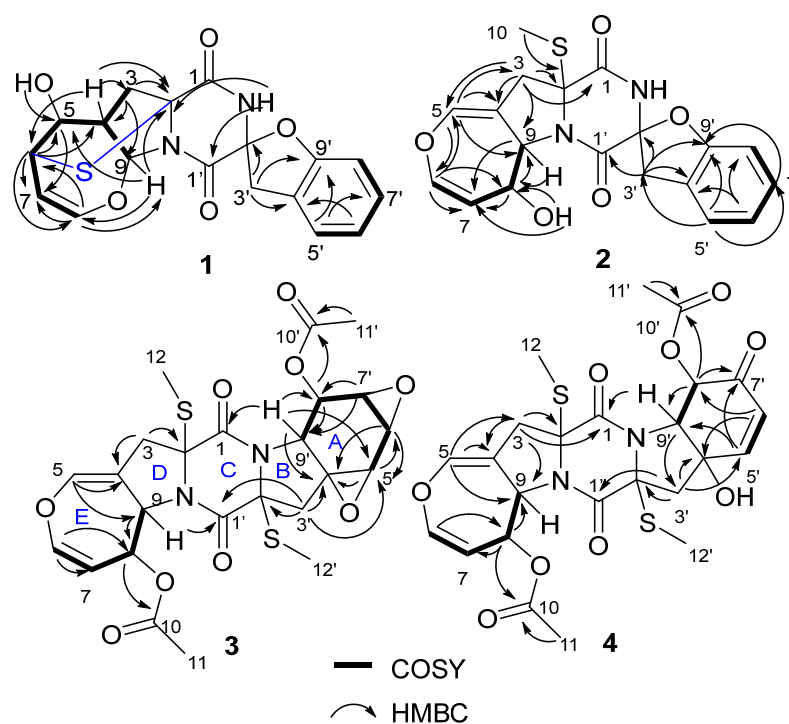
Table 1. ^1H NMR data of compounds **1–6** (700 MHz, δ_{H} in ppm, J in Hz) in DMSO- d_6 .

No.	1	2	3	4	5	6
3	2.21 (d, 12.7), 2.71 (dd, 12.7, 6.5)	2.91 (dt, 15.3, 1.2), 3.14 (dt, 15.3, 2.2)	2.96 (dt, 15.2, 1.2) 3.25 (dt, 15.2, 2.3)	2.92 (dd, 16.1, 2.1) 3.20 (d, 16.1)	2.96 (dt, 15.4, 1.2) 3.24 (dt, 15.4, 2.3)	3.26 (overlap, m)
4	3.06 (t, 6.5)	-	-	-	-	2.70 (dd, 13.6, 5.2), 3.05 (dd, 13.6, 4.5)
5	3.87 (d, 6.5)	6.69 (t, 2.4)	6.76 (t, 2.6)	6.81 (t, 2.6)	6.77 (t, 2.2)	-
6	4.86 (ddd, 7.8, 6.5, 1.2)	6.29 (dd, 8.2, 2.4)	6.43 (dd, 8.3, 2.6)	6.43 (dd, 8.2, 2.6)	6.42 (dd, 8.2, 2.0)	7.19 (overlap, m)
7	4.82 (ddd, 7.8, 6.5, 1.2)	4.79 (dd, 8.2, 2.1)	4.70 (dd, 8.3, 2.2)	4.69 (dd, 8.2, 2.2)	4.72 (dd, 8.2, 2.0)	7.26 (overlap, m)
8	6.00 (d, 6.5)	4.46 (ddt, 7.7, 6.7, 2.1)	5.57 (dt, 8.1, 2.2)	5.52 (dt, 8.2, 2.2)	5.54 (dt, 8.2, 2.1)	7.18 (overlap, m)
9	6.61 (d, 6.5)	4.74 (dq, 7.7, 2.1)	4.92 (dq, 8.1, 2.2)	5.00 (dq, 8.2, 2.2)	4.99 (dq, 8.2, 2.1)	7.26 (overlap, m)
10	-	2.29 (s)	-	-	-	7.19 (overlap, m)
11	-	-	2.01 (s)	1.97 (s)	1.95 (s)	-
12	-	-	2.13 (s)	2.18 (s)	2.15 (s)	-
3'	3.26 (d, 16.4), 3.94 (d, 16.4)	3.25 (d, 16.6), 4.01 (d, 16.6)	2.43 (d, 14.4) 2.85 (d, 14.4)	2.94 (d, 15.4) 3.16 (dd, 15.4, 2.1)	3.30 (overlap, m) 3.45 (dt, 15.9, 1.3)	-
4'	-	-	-	-	-	2.84 (d, 13.1), 3.28 (d, 13.1)
5'	7.26 (d, 7.5)	7.26 (d, 7.5)	3.83 (d, 2.7)	6.98 (d, 10.3)	6.86 (t, 2.2)	-
6'	6.92 (t, 7.5)	6.91 (t, 7.5)	3.67 (dd, 4.3, 2.7)	6.09 (d, 10.3)	6.43 (dd, 8.2, 2.0)	7.12 (overlap, m)
7'	7.14 (t, 8.0)	7.14 (t, 8.0)	3.34 (dd, 4.3, 1.2)	-	4.68 (dd, 8.2, 2.0)	7.24 (overlap, m)
8'	6.81 (d, 8.0)	6.79 (d, 8.0)	5.79 (dd, 9.1, 1.2)	5.73 (d, 11.2)	5.52 (dt, 8.2, 2.2)	7.26 (overlap, m)
9'	-	-	4.34 (d, 9.1)	4.92 (dd, 11.2, 1.5)	4.95 (dq, 8.2, 2.2)	7.24 (overlap, m)
10'	-	-	-	-	-	7.12 (overlap, m)
11'	-	-	1.96 (s)	2.07 (s)	1.97 (s)	1.37 (s)
12'	-	-	2.25 (s)	2.16 (s)	2.47 (s)	-
NH	10.06 (s)	9.77 (s)	-	-	-	-
1-NH	-	-	-	-	-	8.66 (s)
1'-NH	-	-	-	-	-	8.23 (d, 2.0)
5-OH	5.31 (s)	-	-	-	-	-
8-OH	-	5.28 (d, 6.7)	-	-	-	-
4'-OH	-	-	-	6.18 (s)	-	-

The relative configuration of **1** was elucidated by analysis of the NOESY spectrum (Figure S6). The NOE correlations of H-4 with OH-5 and H-9, H-9 with H-3 (δ_{H} 2.71) and H-4, and H-6 with H-4 (Figure 3), indicated their cofacial β -orientations. The NOE correlation of H-5 with H_a-3 (δ_{H} 2.21) indicated their cofacial α -orientations. The NOE correlations from H-5 to H₂-3' revealed their cofacial orientations and the CH₂-3' group at the axial position. The coupling constant of $J_{\text{H-7-H-8}} = 6.5$ Hz indicated that the double bond was a Z-configuration. The absolute configuration of **1** was further determined by electronic circular dichroism (ECD) calculations. The calculated ECD spectrum of (2R, 4S, 5S, 6S, 9R, 2'S)-**1** showed similarity to the experimental ECD spectrum of **1** (Figure 4), which confirmed that the absolute configuration of **1** was 2R, 4S, 5S, 6S, 9R, 2'S.

Table 2. ^{13}C NMR data of compounds 1–6 (175 MHz, δ_{C} in ppm) in $\text{DMSO-}d_6$.

No.	1	2	3	4	5	6
1	165.2, C	166.4, C	163.5, C	164.3, C	163.7, C	-
2	70.8, C	69.2, C	70.1, C	70.8, C	70.7, C	166.2, C
3	48.2, CH ₂	40.2, CH ₂	38.7, CH ₂	40.0, CH ₂	39.0, CH ₂	54.8, C
4	46.3, CH	109.1, C	110.7, C	110.4, C	110.9, C	37.2, CH ₂
5	69.9, CH	136.7, CH	137.0, CH	137.6, CH	137.1, CH	135.9, C
6	52.5, CH	137.9, CH	139.9, CH	139.8, CH	139.9, CH	130.5, CH
7	100.6, CH	111.0, CH	105.3, CH	105.8, CH	105.5, CH	128.0, CH
8	144.9, CH	71.2, CH	71.2, CH	71.5, CH	71.2, CH	126.6, CH
9	92.9, CH	64.1, CH	59.8, CH	59.6, CH	59.6, CH	128.0, CH
10	-	13.3, CH ₃	169.6, C	169.4, C	169.4, C	130.5, CH
11	-	-	20.7, CH ₃	20.8, CH ₃	20.9, CH ₃	-
12	-	-	13.8, CH ₃	14.1, CH ₃	13.9, CH ₃	-
1'	162.8, C	163.4, C	163.6, C	163.1, C	164.3, C	-
2'	91.8, C	93.0, C	71.7, C	69.2, C	74.9, C	164.8, C
3'	38.3, CH ₂	38.4, CH ₂	39.0, CH ₂	48.0, CH ₂	37.6, CH ₂	68.2, C
4'	125.4, C	125.5, C	60.9, C	75.5, C	110.6, C	44.4, CH ₂
5'	124.5, CH	124.5, C	53.6, CH	150.2, CH	137.3, CH	135.0, C
6'	121.3, CH	121.2, CH	47.9, CH	125.8, CH	139.9, CH	130.3, CH
7'	128.1, CH	128.0, CH	54.1, CH	191.5, C	105.5, CH	128.0, CH
8'	109.1, CH	109.1, CH	72.6, CH	74.8, CH	70.7, CH	127.1, CH
9'	156.6, C	156.7, CH	57.5, CH	69.1, CH	60.1, CH	128.0, CH
10'	-	-	169.4, C	168.9, C	169.5, C	130.3, CH
11'	-	-	20.6, CH ₃	20.3, CH ₃	20.7, CH ₃	11.2, C
12'	-	-	14.3, CH ₃	13.8, CH ₃	24.1, CH ₃	-



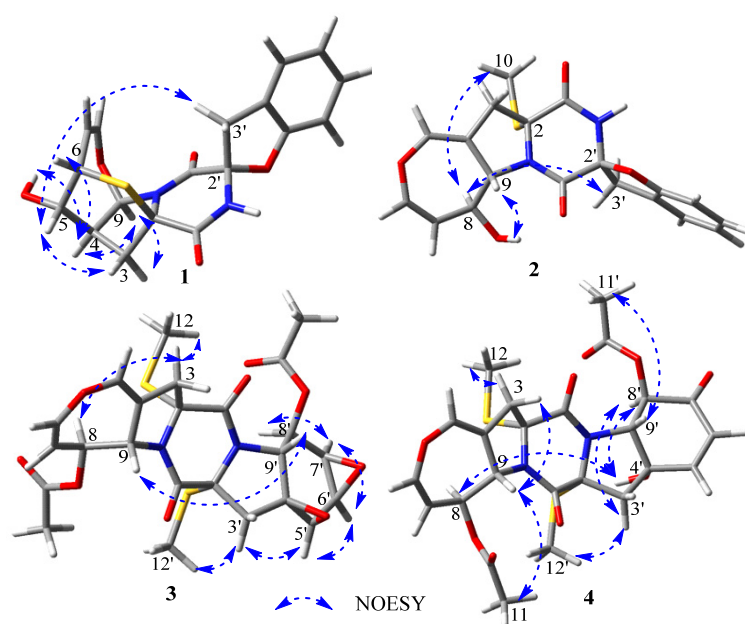


Figure 3. Key NOESY correlations of compounds 1–4.

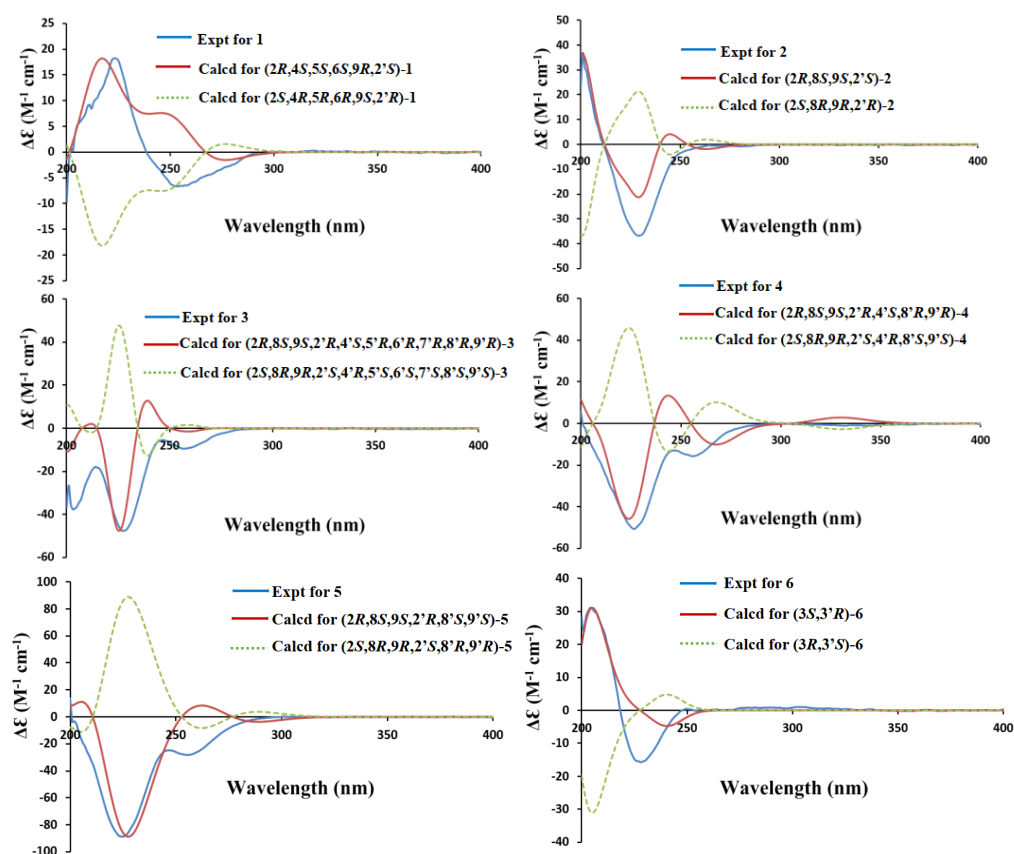


Figure 4. Comparison of experimental and calculated ECD spectra of 1, 2, 4–6 in MeOH and 3 in CH₃CN.

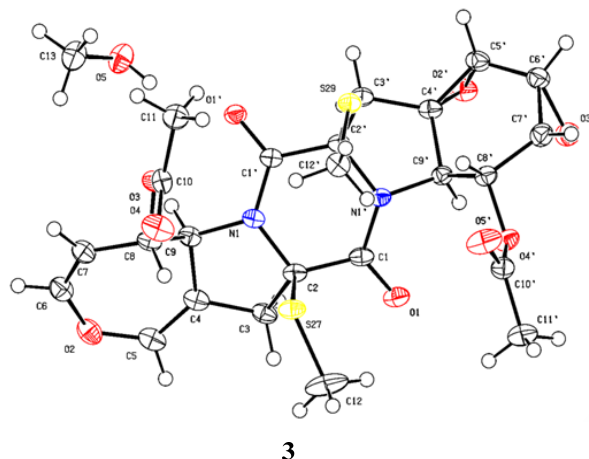
A possible biosynthetic pathway of **1** is shown in Figure S66 [5,8]. The biosynthetic pathway of **1** likely starts with the cyclodipeptide (I) composed of two phenylalanines followed by oxidation to afford the key intermediate II, which could be transferred to III by dehydration and oxidation. Then cyclization and oxidation of III via intermediate IV could

produce V. Finally, V could be translated into compound **1** by further oxidation, cyclization, and sulfurization.

Lecanicillium B (**2**) was obtained as a white powder with the molecular formula $C_{19}H_{18}N_2O_5S$ as determined by HRESIMS ($[M + H]^+ m/z$ 387.1009) and NMR data. The 1H and ^{13}C NMR spectra of **2** (Tables 1 and 2) showed similarity to those of spirobrocazine A [5]. The obvious difference between them was the chemical shift changes of C-4, C-5, C-6, C-7, C-8, and C-9 (δ_C 134.1 (C), 120.3 (CH), 124.0 (CH), 131.6 (CH), 75.1 (CH), and 70.4 (CH) in spirobrocazine A [5], and correspondingly δ_C 109.1 (C), 136.7 (CH), 137.9 (CH), 111.0 (CH), 71.2 (CH) and 64.1 (CH) in **2**, respectively). The COSY spectrum (Figure 2) showing the sequential correlations of H-6/H-7/H-8/H-9, and the HMBC spectrum (Figure 2) showing correlations from H-5 (δ_H 6.69, 1H , t, $J = 2.4$ Hz) to C-3 (δ_C 40.2), C-4 (δ_C 109.1), C-6 (δ_C 137.9), C-9 (δ_C 64.1), from H-6 (δ_H 6.29, 1H , dd, $J = 8.2, 2.4$ Hz) to C-5 (δ_C 136.7), C-7 (δ_C 111.0), C-8 (δ_C 71.2), from H-8 (δ_H 4.46, 1H , ddt, $J = 7.7, 6.7, 2.1$ Hz) to C-7, C-9, from OH-8 (δ_H 5.28, d, $J = 6.7$ Hz) to C-8, and from H-3 [δ_H 2.91 (1H , dt, $J = 15.3, 1.2$ Hz), 3.14 (1H , dt, $J = 15.3, 2.2$ Hz)] to C-2 (δ_C 69.2), C-4, C-5, C-9, suggested that the E ring in **2** was a seven-membered 4,5-dihydrooxepine ring, as shown, instead of a six-membered ring. The coupling constant of $J_{H-6-H-7} = 8.2$ Hz indicated that the double bond was a Z-configuration. In addition, the NOESY spectrum of **2** (Figure S15) also showed great similarity to that of spirobrocazine A. The NOE correlation of OH-8 with H-9 indicated their cofacial β -orientations, while the NOE correlations of H-8 with H₃-10 and H_a-3' (δ_H 4.01) indicated their cofacial α -orientations and the CH₂-3' group at the axial position (Figure 3). Furthermore, the calculated ECD spectrum of (2*R*, 8*S*, 9*S*, 2'*S*)-**2** showed similarity to the experimental ECD spectrum of **2** (Figure 4), indicating the absolute configuration of **2**, as shown.

Lecanicillium C (**3**) was isolated as a white powder with the molecular formula $C_{24}H_{26}N_2O_9S_2$ as determined by HRESIMS ($[M + Na]^+ m/z$ 573.0969) and NMR. The 1H and ^{13}C NMR spectra of **3** (Tables 1 and 2) showed similarity to those of bisdethiobis(methylsulfanyl)acetylpoaranotin [8]. The obvious difference between them was the additional presence of three tertiary methine signals (δ_H 3.83 (1H , d, $J = 2.7$ Hz), 3.67 (1H , dd, $J = 4.3, 2.7$ Hz), 3.34 (1H , dd, $J = 4.3, 1.2$ Hz); δ_C 54.1, 53.6, 47.9) and one oxygenated nonprotonated carbon (δ_C 60.9), and the disappearance of the signals for two double bonds in **3**. Detailed analysis of HSQC, HMBC and COSY spectra (Figure 2, Figures S21–S23) proved that **3** contained the same structural parts of rings B–E as those of bisdethiobis(methylsulfanyl)acetylpoaranotin. Furthermore, the COSY spectrum (Figure 2) showed correlations from H-5' (δ_H 3.83, 1H , d, $J = 2.7$ Hz) to H-6' (δ_H 3.67, 1H , dd, $J = 4.3, 2.7$ Hz), from H-6' to H-7' (δ_H 3.34, 1H , dd, $J = 4.3, 1.2$ Hz), and from H-8' (δ_H 5.79, 1H , dd, $J = 9.1, 1.2$ Hz) to H-7' and H-9' (δ_H 4.34, 1H , d, $J = 9.1$ Hz), and the HMBC spectrum (Figure 2) showed correlations from H-5' to C-4' (δ_C 60.9) and C-6' (δ_C 47.9), from H-6' to C-4', C-5' (δ_C 53.6), from H-7' to C-8' (δ_C 72.6), C-9' (δ_C 57.5), from H-8' to C-9', C-10' (δ_C 169.4), from H-9' to C-1 (δ_C 163.5), C-4', C-5', C-8', from H-3' [δ_H 2.85 (1H , d, $J = 14.4$ Hz), 2.43 (1H , d, $J = 14.4$ Hz)] to C-1' (δ_C 163.6), C-2' (δ_C 71.7), C-4', C-5', and from H₃-11' to C-10'. Combining with the molecular formula, these above data suggested that the A ring was a six-membered ring with an acetyl group attached at C-8' and two oxygenated three-membered rings between C-4' and C-5', and between C-6' and C-7', respectively. The small coupling constants of $J_{H-5'-H-6'}$ (2.7 Hz), $J_{H-6'-H-7'}$ (4.3 Hz), and $J_{H-7'-H-8'}$ (1.2 Hz) suggested a *cis*-diaxial relationship between H-5' and H-6', between H-6' and H-7', and between H-7' and H-8', respectively. NOE correlations of H-5' with H-6', H-6' with H-7' and H-7' with H-8' also indicated H-5', H-6', H-7', and H-8' on the same face. The large coupling constants of $J_{H-8-H-9}$ (8.1 Hz) and $J_{H-8'-H-9'}$ (9.1 Hz) suggested a *trans*-diaxial relationship between H-8 and H-9, and between H-8' and H-9', respectively. Furthermore, the NOE correlations of H-3 (δ_H 3.25) with H-8 and H₃-12 indicated the assignment of α -orientation for H-8 and H₃-12, NOE correlations of H-3' (δ_H 2.43) with H-5' and H₃-12' indicated α -orientation for H₃-12' and H-5', and NOE correlations of H-9 with H-9' indicated β -orientation for H-9 and H-9' (Figure 3). Thus, the structure of **3** was inferred as shown. The absolute

configuration of **3** was determined as $2R, 8S, 9S, 2'R, 4'S, 5'R, 6'R, 7'R, 8'R, 9'R$ by a single crystal X-ray diffraction analysis using Cu $K\alpha$ radiation (Figure 5), which was supported by the calculated ECD spectrum of $(2R, 8S, 9S, 2'R, 4'S, 5'R, 6'R, 7'R, 8'R, 9'R)$ -**3** showing agreement with the experimental ECD spectrum of **3** (Figure 4).



3

Figure 5. ORTEP plot of the X-ray crystallographic data for **3**.

Lecanicillium D (**4**) was isolated as a white solid with the molecular formula $C_{24}H_{26}N_2O_9S_2$ as determined by HRESIMS ($[M + NH_4]^+$ m/z 568.1408). The 1H and ^{13}C NMR spectra of **4** (Tables 1 and 2) showed similarity to those of **3**. The obvious difference between them was the presence of an α, β -unsaturated ketone group (δ_H 6.98 (1H , d, $J = 10.3$ Hz), 6.09 (1H , d, $J = 10.3$ Hz); δ_C 191.5, 150.2, 125.8) and the disappearance of three tertiary methine signals in **4**. The HMBC spectrum (Figure 2) showing correlations from H-5' (δ_H 6.98, 1H , d, $J = 10.3$ Hz) to C-7' (δ_C 191.5) and C-9' (δ_C 69.1), from H-6' (δ_H 6.09, 1H , d, $J = 10.3$ Hz) to C-8' (δ_C 74.8) and C-4' (δ_C 75.5), from H-8' (δ_H 5.73, 1H , d, $J = 11.2$ Hz) to C-7' and C-10', from H-3' [δ_H 2.94 (1H , d, $J = 15.4$ Hz), 3.16 (1H , dd, $J = 15.4, 2.1$ Hz)] to C-4' and C-5', and from H₃-11' to C-10', and the COSY spectrum (Figure 2) showing correlations from H-5' to H-6', and from H-8' to H-9', revealed the existence of an α, β -unsaturated ketone instead of two oxygenated three-membered rings in **4**. The NOE correlation of H-9 with H₃-11 suggested the assignment of α -orientation for H-8 and β -orientation for H-9, and the NOE correlations of H-3 (δ_H 2.92) with H-9, and H-3 (δ_H 3.20) with H₃-12 indicated H₃-12 was α -oriented. The 11.2 Hz coupling constant between H-8' and H-9' and the NOE correlation of H-9' with H₃-11' suggested the assignment of α -orientation for H-8' and β -orientation for H-9'. The NOE correlation of OH-4' with H-8' indicated their cofacial α -orientations. The NOE correlations of H-3' (δ_H 2.94) with H-8' and H₃-12' indicated H₃-12' was also α -oriented. The NOE correlations of H-8 with OH-4' indicated that H-8 and OH-4' were α -orientated. The absolute configuration of **4** was further determined by ECD calculation. The great similarity between the experimental ECD spectrum of **4** and the calculated ECD spectrum of $(2R, 8S, 9S, 2'R, 4'S, 8'R, 9'R)$ -**4** (Figure 4) indicated the absolute configuration of **4** as shown.

Lecanicillium E (**5**) was obtained as a white powder with the molecular formula $C_{24}H_{26}N_2O_8S_3$ as determined by HRESIMS ($[M + NH_4]^+$ m/z 584.1189). The 1H and ^{13}C NMR spectra of **5** (Tables 1 and 2) showed great similarity to those of bisdithio-bis(methylthio)acetylaranotin [8]. The only obvious difference between them was the down-field shifts of H₃-12' (δ_H 2.47, 1H , s), C-12' (δ_C 24.1) and C-2' (δ_C 74.9) in **5**. Combined with the molecular formula, these data indicated a disulfide methyl attached at C-2' instead of a sulfide methyl in **5**. Combined with the coupling constants of $J_{H-8'-H-9'}$ and $J_{H-8-H-9}$ (both 8.2 Hz), the NOE correlations of H-8 with H₃-12, H-9 with H₃-11, H-8' with H₃-12', and H-9' with H₃-11' indicated that H-8, H-8', H₃-12', H₃-12 were α -oriented, and H-9, H-9', H₃-11', H₃-11 were β -oriented (Figure S65). The absolute configuration of **5** was determined as shown by comparing the experimental ECD spectrum of **5** and the calculated

ECD spectrum of (2*R*, 8*S*, 9*S*, 2'*R*, 8'*S*, 9'*S*)-**5** (Figure 4), which was further supported by the great similarity of the ECD spectra of **5** with bisdethiobis(methylthio)acetylaranotin [24].

Lecanicillium F (**6**) was isolated as a white solid with the molecular formula C₁₉H₂₀N₂O₂S as determined by HRESIMS ([M + H]⁺ *m/z* 341.1316). The ¹H and ¹³C NMR spectra of **6** (Tables 1 and 2) exhibited great similarity to those of emethacin B [17]. The only obvious difference between them was the disappearance of a sulfide methyl and the additional presence of a methine (δ_C 54.8, δ_H 3.26) instead of a nonprotonated carbon in **6**. The COSY correlations of δ_H 3.26 with H-4 and NH-1' (δ_H 8.23), and the HMBC correlations from δ_H 3.26 to C-2 (δ_C 166.2), C-4 (δ_C 37.2), C-5 (δ_C 135.9), from NH-1 (δ_H 8.66) to C-2' (δ_C 164.8), C-3' (δ_C 68.2), C-4' (δ_C 44.4), and from NH-1' to C-2, C-3' (Figure S63), suggested the methine was C-3 (δ_C 54.8, δ_H 3.26) in **6**. The NOE correlations of H-3 with H₃-11', and H-4 (δ_H 2.70) with H-4' (δ_H 3.28) (Figure S65) indicated the cofacial orientations for H-3 and H₃-11', and H-4 (δ_H 2.70) and H-4' (δ_H 3.28), respectively. The similarity between the experimental ECD spectrum of **6** and the calculated ECD spectrum of (3*S*,3'*R*)-**6** (Figure 4) indicated the absolute configuration of **6** as shown.

Compounds **2–19** were tested for their cytotoxicity towards human lung adenocarcinoma cell line H1975 and human hepatocellular carcinoma cell line HepG-2, and toxicity towards brine shrimps. The cytotoxicity results (Table 3) showed that **5**, **7**, and **16** displayed significant cytotoxicity against H1975, with IC₅₀ values of 7.2~16.9 μM, **4**, **11**, **17**, and **18** displayed mild cytotoxicity against H1975, with IC₅₀ values of 35.2~71.5 μM; only **18** had mild cytotoxicity against HepG-2, with an IC₅₀ value of 41.2 μM. The results indicated that the disulfide bond unit in **5** was an active group for its cytotoxicity, which is consistent with the conclusions reported in the literatures [25,26]. A comparison of the structures and cytotoxicities of **6**, **7**, and **19** suggested that lacking thiomethyl and benzene could significantly decrease the cytotoxicity of this type of alkaloids. In addition, a comparison of the structures and cytotoxicity of **2**, **3**, **4**, **11**, and **16** suggests the skeleton of A/B/C ring fragment also could significantly affect the cytotoxicity of this type of alkaloids. Furthermore, brine shrimp lethality assays (Table 3) showed that only **4** and **15** exhibited medium toxicity, with TC₅₀ values of 40–50 μM, towards brine shrimps.

Table 3. Antibacterial activities, cytotoxicity, and toxicity of 1–19.

Comp.	Antibacterial Activity (MIC: μg/mL)								Cytotoxicity (IC ₅₀)	against (μM)	Toxicity (TC ₅₀ in μg/mL)
	<i>B. subtilis</i>	<i>M. luteus</i>	<i>E. coli</i>	<i>S. aureus</i>	MRSA	<i>S. agalactiae</i>	<i>P. aeruginosa</i>	<i>S. imiae</i>			
1	60	>80	>80	>80	>80	>80	>80	>80	-	-	>80
2	80	60	>80	>80	>80	>80	>80	70	>80	>80	>80
3	>80	>80	>80	>80	>80	>80	>80	>80	>80	>80	>80
4	50	>80	>80	>80	>80	>80	>80	40	71.5	>80	80
5	10	40	80	>80	>80	25	>80	15	16.3	>80	40
6	>80	>80	>80	>80	>80	>80	>80	>80	>80	>80	-
7	>80	>80	>80	>80	>80	>80	>80	>80	16.9	>80	-
8	>80	>80	>80	>80	>80	>80	>80	>80	>80	>80	-
9	>80	>80	>80	>80	>80	>80	>80	>80	>80	>80	>80
10	>80	>80	>80	>80	>80	>80	>80	>80	>80	>80	>80
11	60	>80	>80	>80	>80	>80	>80	50	69.3	>80	>80
12	>80	50	>80	>80	>80	50	>80	>80	>80	>80	50
13	>80	>80	>80	>80	>80	>80	>80	>80	>80	>80	-
14	>80	>80	>80	>80	>80	>80	>80	40	>80	>80	>80
15	80	>80	>80	>80	>80	>80	>80	>80	>80	>80	>80
16	70	>80	>80	>80	>80	70	>80	>80	7.2	>80	-
17	80	>80	>80	>80	>80	70	>80	30	35.2	>80	-
18	80	>80	>80	>80	>80	>80	>80	40	50.6	41.2	>80
19	80	70	>80	>80	>80	>80	>80	>80	>80	>80	-
VMN	-	0.6	-	-	2.5	-	-	-	-	-	-
CFN	0.6	-	0.6	0.6	-	5	0.6	2.5	-	-	-

VMN: Vancomycin; CFN: Ciprofloxacin; “-”: Not tested.

Compounds 1–19 were also evaluated for their antibacterial activity towards eight pathogens: *Bacillus subtilis*, *Micrococcus luteus*, *Escherichia coli*, *Staphylococcus aureus*, *S. aureus* MRSA, *Streptococcus agalactiae*, *S. iniae*, and *Pseudomonas aeruginosa*. Antibacterial assays (Table 3) exhibited that only 5 had significant antibacterial activity against *B. subtilis*, *M. luteus*, *S. agalactiae*, and *S. iniae*, with MIC values of 10–40 µg/mL. Other compounds showed mild or no obvious antibacterial activity. The results indicated that a disulfide bond unit at C-2' was crucial for the antibacterial activity of this type of alkaloids.

3. Experimental Section

3.1. General Experimental Procedure

UV spectra were measured using a UV-2600 spectrophotometer (Shimadzu). IR spectra were obtained on an IR Affinity-1 Fourier transform infrared spectrophotometer (Shimadzu, Kyoto, Japan). ECD spectra were acquired on a Chirascan circular dichroism spectrometer (Applied Photophysics Ltd., Graz, Austria). Optical rotations were recorded using a MCP 500 polarimeter (Anton Paar). Melting points were recorded with a digital display microscopic melting point instrument (SGW X-5). NMR data were acquired with a Bruker AVANCE III HD 700 MHz NMR spectrometer (Bruker) with TMS as reference. HRESIMS spectroscopic data were obtained on a MaXis quadrupole-time-of-flight mass spectrometer (Bruker, Karlsruhe, Germany). Preparative reversed-phase HPLC was performed on a Shimadzu LC-20A preparative liquid chromatography system with a YMC-Pack ODS column (250 × 20 mm, S-5 µm, 12 nm). Sephadex LH-20 (GE Healthcare) was used for the chromatographic column (CC). RP-MPLC (reversed-phase-medium pressure preparative liquid chromatography) was carried out using the CHEETAH MP200 system (Agela Technologies, Tianjin, China) and Claricep Flash columns filled with ODS (40–63 µm, YMC). Silica gel (200–300 mesh) for CC and GF254 for TLC were purchased from Yantai Jiangyou Silica Gel Development Co., Ltd. Sea salts were commercially obtained from Guangzhou Hai Li Aquarium Technology Co., Ltd., Guangzhou, China.

3.2. Fungal Material

The fungus *Lecanicillium kalimantanense* was isolated from a mangrove sediment sample collected in the Bailu park, Sanya city, Hainan province. The strain was identified as *Lecanicillium kalimantanense* by internally transcribed spacer (ITS) region sequence data of the rDNA and given the Genbank accession number KM264285. The fungus *L. kalimantanense* was deposited in the RNAM Center, South China Sea Institute of Oceanology, Chinese Academy of Science.

3.3. Fermentation and Extraction

The spores of the fungus *L. kalimantanense* were added to 5 × 500 mL Erlenmeyer flasks, each containing 200 mL potato dextrose (PD) medium, and fermented for 3 days at 28 °C. Then 3 mL of spore suspension was transferred into 267 × 1 L Erlenmeyer flasks, each containing 300 mL culture media (glucose 1%, D-mannitol 2%, maltose 2%, corn meal 0.05%, monosodium glutamate 1%, KH₂PO₄ 0.05%, MgSO₄·7H₂O 0.03%, yeast extract 0.3%, sea salt 3%). Static fermentation was performed for 26 days at 28 °C. After fermentation, the broth and mycelia were separated with gauze. The broth was extracted with EtOAc to obtain crude extract (28.9 g). The mycelia were extracted three times with acetone, and further extracted three times with EtOAc to yield a crude extract (58.3 g). Then the two crude extracts (28.9 g and 58.3 g) were combined for further isolation.

3.4. Isolation and Purification

The combined crude extract (87.2 g) was fractionated on a normal-phase column using a stepped gradient elution with CH₂Cl₂/MeOH (*v/v*, 100:0, 98:2, 95:5, 90:10, 85:15, 80:20, 70:30, 50:50, 0:100) to obtain eight fractions (Fr.1–Fr.8). Fr.3 (10.9 g) was separated with Sephadex LH-20 eluting with CH₂Cl₂/MeOH (1:1) to obtain eleven subfractions (Fr.3.1–Fr.3.11). Fr.3.3 was further purified by HPLC eluting with MeOH/H₂O (*v/v* 7:3,

3 mL/min) to give **12** (9.0 mg, t_R = 13.0 min). Fr.3.4 was further purified by HPLC eluting with MeOH/H₂O (*v/v* 6:4, 3 mL/min) to give **8** (3.5 mg, t_R = 29.0 min), **10** (11.0 mg, t_R = 22.0 min), and **13** (9.0 mg, t_R = 19.0 min). Fr.3.5 was further purified by HPLC eluting with MeOH/H₂O (*v/v* 55:45, 3 mL/min) to give **5** (1.7 mg, t_R = 43.0 min), **7** (1.1 mg, t_R = 35.5 min), and **15** (2.6 mg, t_R = 44.0 min). Fr.3.9 was further purified by HPLC eluting with MeOH/H₂O (*v/v* 7:3, 3 mL/min) to give **9** (20.0 mg, t_R = 10.0 min). Then Fr.3.6–Fr.3.8 were combined and further separated by ODS column eluting with MeOH/H₂O (*v/v* 10:90–100:0) to obtain subfractions (Fr.3.6.1–Fr.3.6.22). Fr.3.6.6 was purified by HPLC eluting with MeOH/H₂O (*v/v* 42.5:57.5, 2.5 mL/min) to give **6** (2.3 mg, t_R = 32.0 min). Fr.3.6.8 was purified by HPLC eluting with MeOH/H₂O (*v/v* 55:45, 2.5 mL/min) to give **3** (1.6 mg, t_R = 26.0 min), **2** (1.5 mg, t_R = 30.0 min), and **4** (2.6 mg, t_R = 24.0 min). Fr.3.2.10 was purified by HPLC eluting with MeOH/H₂O (*v/v* 58.5:41.5, 3 mL/min) to give **14** (3.0 mg, t_R = 33.0 min). Fr.3.6.12 was purified by HPLC eluting with MeOH/H₂O (*v/v* 59:41, 3 mL/min) to give **11** (6.5 mg, t_R = 40.0 min) and **18** (3.4 mg, t_R = 45.0 min). Fr.3.6.15 was further purified by HPLC eluting with MeOH/H₂O (*v/v* 6:4, 2.5 mL/min) to give **16** (0.8 mg, t_R = 75.0 min) and **17** (1.4 mg, t_R = 68.0 min). Fr.4 (8.6 g) was separated with Sephadex LH-20 eluting with CH₂Cl₂/MeOH (1:1) to obtain eleven subfractions (Fr.4.1–Fr.4.3). Fr.4.2 was further separated by ODS column eluting with MeOH/H₂O (*v/v* 10:90–100:0) to obtain subfractions (Fr.4.2.1–Fr.4.2.33). Fr.4.2.8 was purified by HPLC eluting with MeOH/H₂O (*v/v* 9:11, 3 mL/min) to give **19** (2.0 mg, t_R = 20.0 min). Fr.4.2.10 was purified by HPLC eluting with MeOH/H₂O (*v/v* 9:11, 3 mL/min) to give **1** (1.5 mg, t_R = 26.0 min).

Lecanicillium A (**1**). White powder; $[\alpha]_D^{25}$ −86 (*c* 0.10, MeOH); UV (MeOH) λ_{max} (log ϵ) 212 (4.30), 277 (3.70), 283 (3.60) nm; ECD (0.33 mM, MeOH) λ_{max} ($\Delta\epsilon$) 200 (−9.00), 223 (16.86), 258 (−6.02) nm; IR (film) ν_{max} 3746, 3433, 3267, 2922, 2855, 2365, 2322, 2257, 1676, 1458, 1389, 1236, 1190, 1109, 1084, 1022, 995, 862, 760, 644, 596 cm^{−1}; ¹H and ¹³C NMR data, Tables 1 and 2; HR-ESIMS *m/z* 373.0851 [M + H]⁺ (calcd for C₁₈H₁₇N₂O₅S, 373.0853).

Lecanicillium B (**2**). White powder; $[\alpha]_D^{25}$ −168 (*c* 0.10, MeOH); UV (MeOH) λ_{max} (log ϵ) 210 (4.30), 276 (3.53), 283 (3.47) nm; ECD (0.32 mM, MeOH) λ_{max} ($\Delta\epsilon$) 200 (21.64), 201 (34.30), 229 (−34.46) nm; IR (film) ν_{max} 3341, 2922, 2841, 1676, 1649, 1545, 1514, 1460, 1410, 1113, 1018, 671, 598 cm^{−1}; ¹H and ¹³C NMR data, Tables 1 and 2; HR-ESIMS *m/z* 387.1009 [M + H]⁺ (calcd for C₁₉H₁₉N₂O₅S, 387.1009).

Lecanicillium C (**3**). colorless crystals; mp 172–174 °C; $[\alpha]_D^{25}$ −213 (*c* 0.10, CH₃CN); UV (CH₃CN) λ_{max} (log ϵ) 206 (4.50) nm; ECD (0.45 mM, CH₃CN) λ_{max} ($\Delta\epsilon$) 200 (−24.56), 201 (−17.74), 203 (−25.16), 214 (−11.98), 227 (−31.84), 247 (−3.68), 257 (−6.35) nm; IR (film) ν_{max} 3861, 3744, 3618, 2922, 2853, 1738, 1674, 1514, 1377, 1236, 1194, 1138, 1034, 972, 731, 648, 602 cm^{−1}; ¹H and ¹³C NMR data, Tables 1 and 2; HR-ESIMS *m/z* 573.0969 [M + Na]⁺ (calcd for C₂₄H₂₆N₂NaO₉S₂, 573.0972).

Lecanicillium D (**4**). White powder; $[\alpha]_D^{25}$ −206 (*c* 0.10, MeOH); UV (MeOH) λ_{max} (log ϵ) 207 (4.35) nm; ECD (0.45 mM, MeOH) λ_{max} ($\Delta\epsilon$) 200 (3.58), 226 (−33.79), 247 (−8.64), 256 (−10.55) nm; IR (film) ν_{max} 3331, 2945, 2920, 2841, 1740, 1659, 1535, 1514, 1460, 1398, 1113, 1018, 671, 598 cm^{−1}; ¹H and ¹³C NMR data, Tables 1 and 2; HR-ESIMS *m/z* 568.1408 [M + NH₄]⁺ (calcd for C₂₄H₃₀N₃O₉S₂, 568.1418).

Lecanicillium E (**5**). White powder; $[\alpha]_D^{25}$ −282 (*c* 0.10, MeOH); UV (MeOH) λ_{max} (log ϵ) 207 (4.36) nm; ECD (0.44 mM, MeOH) λ_{max} ($\Delta\epsilon$) 200 (9.37), 202 (−2.30), 225 (−61.07), 247 (−17.03), 256 (−19.43) nm; IR (film) ν_{max} 3347, 2951, 2924, 2843, 1734, 1670, 1375, 1302, 1236, 1192, 1130, 1018, 669, 598 cm^{−1}; ¹H and ¹³C NMR data, Tables 1 and 2; HR-ESIMS *m/z* 584.1189 [M + NH₄]⁺ (calcd for C₂₄H₃₀N₃O₈S₃, 584.1190).

Lecanicillium G (**6**). White powder; $[\alpha]_D^{25}$ −5 (*c* 0.10, MeOH); UV (MeOH) λ_{max} (log ϵ) 206 (4.08) nm; ECD (0.44 mM, MeOH) λ_{max} ($\Delta\epsilon$) 200 (−19.33), 201 (16.40), 204 (21.49), 228 (−10.86) nm; IR (film) ν_{max} 3354, 2943, 2833, 1670, 1653, 1558, 1541, 1506, 1472, 1456, 1418, 1115, 1020, 667, 599 cm^{−1}; ¹H and ¹³C NMR data, Tables 1 and 2; HR-ESIMS *m/z* 341.1316 [M + H]⁺ (calcd for C₁₉H₂₁N₂O₂S, 341.1318).

3.5. X-ray Crystallographic Analysis of **3**

Crystallographic data were collected on a Rigaku MicroMax 007 diffractometer (Rigaku Corporation, Tokyo, Japan) equipped with Cu K α radiation and a graphite monochromator. The structure was solved by direct methods with the SHELXTL and refined by full-matrix, least-squares techniques. Crystallographic data for **3** were deposited with the Cambridge Crystallographic Data Centre as supplementary publication number CCDC 2298244.

Crystal data for **3**: C₂₄H₂₆N₂O₉S₂·CH₃OH, FW = 582.63; colorless crystal from MeOH; crystal size = 0.15 × 0.12 × 0.1 mm³; T = 100.00 (10) K; monoclinic, space group P2₁ (no. 4); unit cell parameters: a = 7.14328(5) Å, b = 16.25526(10) Å, c = 11.41675(7) Å, α = 90°, β = 93.4877(6)°, γ = 90°, V = 1323.211(14) Å³, Z = 2, D_{calc} = 1.462 g/cm³, F(000) = 612.0, μ (CuK α) = 2.357 mm⁻¹; 25678 reflections measured (7.758° ≤ 2 θ ≤ 148.752°), 5292 unique (R_{int} = 0.0323, R_{sigma} = 0.0216), which were used in all calculations. The final R_1 was 0.0242 ($I > 2\sigma(I)$) and wR_2 was 0.0641 (all data). Flack parameter = −0.001(4).

3.6. ECD Calculations

The ECD calculations for **1–6** were performed using the Gaussian 16 program package. The procedures were the same as described in our previous studies [27]. The Spartan 14 program (Wavefunction Inc., Tokyo, Japan) was used for calculating the molecular Merck force field (MMFF). Density functional theory (DFT) and time-dependent density functional theory (TDDFT) calculations were performed using the Gaussian 16 program package. An MMFF model was used for the conformational search, then the conformers with lower relative energies (<10 kcal/mol) were subjected to geometry optimization with the DFT method at the B3LYP/6-31g (d) level in MeOH or CH₃CN. Vibrational frequency calculations were carried out at the same level to evaluate their relative thermal (ΔE) and free energies (ΔG) at 298.15 K. The geometry optimized conformers were further calculated at the M062X/def2TZVP level and the solvent (MeOH or CH₃CN) effects were taken into consideration by using SMD. The optimized conformers with a Boltzmann distribution of more than 1% population were further subjected to ECD calculation, which were performed by TDDFT methodology at the PBE1PBE/6-311g(d) level. The number of excited states was 60 for **1**, **2**, and **6**, 85 for **3** and **4**, and 102 for **5**. The ECD spectra were generated by the software SpecDis using a Gaussian band shape with 0.20–0.30 eV exponential half-width from dipole-length dipolar and rotational strengths. The equilibrium population of each conformer at 298.15 K was calculated from its relative free energies using Boltzmann statistics. The calculated spectra of compounds **1–6** were generated from the low-energy conformers according to the Boltzmann weighting of each conformer in MeOH solution for **1**, **2**, **4**, **5**, and **6** and CH₃CN for **3**, respectively.

3.7. Cytotoxicity

Cytotoxic activity was evaluated using the human lung adenocarcinoma cell line H1975 and human hepatocellular carcinoma cell line HepG-2, using the CCK-8 method as described in our previous study [28]. Briefly, each of the test compounds was dissolved in DMSO and further diluted to give final concentrations of 80, 40, 20, 10, 5, 2.5, and 1.25 μ M, respectively. H1975 cells or HepG-2 cells (5×10^3 cells/plate) were seeded in 96-well plates and treated with compounds at the indicated concentration for 24 hours and then 10 μ L CCK-8 reagent was added to each well. The plates were incubated at 37 °C for another 4 hours. Finally, the optical density was measured at a wavelength of 450 nm with a Bio-Rad microplate reader. Dose–response curves were generated, and the IC₅₀ values were calculated from the linear portion of log dose–response curves.

3.8. Brine Shrimp Lethality Bioassays

The methods were the same as those used in our previous studies [27].

3.9. Antibacterial Assays

The micro broth dilution method [29] was used to evaluate the antibacterial activities of compounds 1–19 against the growth of eight common pathogens: *Bacillus subtilis* BS01, *Micrococcus luteus*, *Escherichia coli* ATCC 25922, *Staphylococcus aureus* ATCC 6538, *S. aureus* MRSA, *Streptococcus agalactiae* ATCC 13813, *S. iniae*, and *Pseudomonas aeruginosa* ATCC 9027 in 96-well polystyrene plates. Vancomycin and ciprofloxacin were used as positive controls. Briefly, wells containing 100 μ L bacteria dilutions ($OD_{600} = 0.01$) in Luria–Bertani (LB) medium were supplemented with different concentrations of 1–19 (80, 40, 20, 10, 5, 2.5, 1.25, and 0.625 μ g/mL), vancomycin, and ciprofloxacin (40, 20, 10, 5, 2.5, 1.25, 0.625, and 0.3125 μ g/mL), respectively. The MICs were determined after 24 hours' incubation at 37 °C with the tested compounds.

4. Conclusions

In summary, six new thiodiketopiperazine-class alkaloids, lecanicilliums A–F (1–6), together with 13 known analogues (7–19) were isolated from the mangrove sediment-derived fungus *L. kalimantanense* SCSIO41702. Lecanicillium A contained an unprecedented 6/5/6/5/7/6 cyclic system with a spirocyclic center at C-2'. Biologically, lecanicillium E, emethacin B, and versicolor A displayed significant inhibitory activity against H1975, with IC_{50} values of 7.2–16.9 μ M, and lecanicillium E also showed antibacterial activities against four pathogens, with MIC values of 10–40 μ g/mL. The cytotoxicity and antibacterial activity results indicated that the disulfide bond unit at C-2' was crucial for the activity of this kind of alkaloids. This finding further clarified the chemical structure diversity of thiodiketopiperazine-class alkaloids, and the structural diversity and biological activities of thiodiketopiperazine-class alkaloids may be worthy of further studies.

Supplementary Materials: The following supporting information can be downloaded at <https://www.mdpi.com/article/10.3390/md21110575/s1>: the 1D NMR, 2D NMR, HRESIMS, IR, and UV spectra of compounds 1–6, details of ECD calculation of compounds 1–6, X-ray crystallographic data for compound 3.

Author Contributions: Performing experiments, data analysis, and writing—original draft preparation, L.-F.Z. and J.L.; testing the activities, L.-X.L. and C.-N.Y.; formal analysis, X.L.; resources, data analysis, writing—review and editing, supervision, and funding acquisition, S.-H.Q. All authors have read and agreed to the published version of the manuscript.

Funding: The authors are grateful for the financial support provided by the National Natural Science Foundation of China (82173709 and 82373756), Key Science and Technology Project of Hainan Province (ZDKJ202018), and the Marine Economy Development Project of Guangdong Province (GDNRC [2023]43).

Institutional Review Board Statement: Not applicable.

Data Availability Statement: The original data presented in the study are included in the article/Supplementary Material; further inquiries can be directed to the corresponding author.

Acknowledgments: The authors also appreciate the analytical facility center (Zhi-Hui Xiao, Xiao-Hong Zheng, Ai-Jun Sun, Xuan Ma, and Yun Zhang) of the South China Sea Institute of Oceanology, Chinese Academy of Sciences, for acquiring NMR, HRESIMS data, experimental ECD data, and X-ray crystallography of these compounds.

Conflicts of Interest: The authors declare that they have no known competing financial interests or personal relationships that could have appeared to influence the work reported in this paper.

References

1. Gardiner, D.M.; Waring, P.; Howlett, B. The epipolythiodioxopiperazine (ETP) class of fungal toxins: Distribution, mode of action, functions and biosynthesis. *J. Microbiol.* **2005**, *151*, 1021–1032. [[CrossRef](#)]
2. Welch, T.R.; Williams, R.M. Epithiodioxopiperazines. occurrence, synthesis and biogenesis. *Nat. Prod. Rep.* **2014**, *31*, 1376–1404. [[CrossRef](#)]

3. Ellen, M.F.; Barbara, J.H. Biosynthetic gene clusters for epipolythiodioxopiperazines in filamentous fungi. *Mycol. Res.* **2008**, *112*, 162–169.
4. Wang, J.M.; Ding, G.Z.; Fang, L.; Dai, J.G.; Yu, S.S.; Wang, Y.H.; Chen, X.G.; Ma, S.G.; Qu, J.; Xu, S.; et al. Thiodiketopiperazines Produced by the Endophytic Fungus *Epicoccum nigrum*. *J. Nat. Prod.* **2010**, *73*, 1240–1249. [[CrossRef](#)]
5. Meng, L.H.; Wang, C.Y.; Mandi, A.; Li, X.M.; Hu, X.Y.; Kassack, M.U.; Kurtan, T.; Wang, B.G. Three Diketopiperazine Alkaloids with Spirocyclic Skeletons and One Bisthiodiketopiperazine Derivative from the Mangrove-Derived Endophytic Fungus *Penicillium brocae* MA-231. *Org. Lett.* **2016**, *18*, 5304–5307. [[CrossRef](#)]
6. Niu, S.W.; Liu, D.; Shao, Z.Z.; Proksch, P.; Lin, W.H. Eutypellazines N–S, new thiodiketopiperazines from a deep sea sediment derived fungus *Eutypella* sp. with anti-VRE activities. *Tetrahedron Lett.* **2017**, *58*, 3695–3699. [[CrossRef](#)]
7. Liu, H.; Fan, J.; Zhang, P.; Hu, Y.C.; Liu, X.Z.; Li, S.M.; Yin, W.B. New insights into the disulfide bond formation enzymes in epidithiodiketopiperazine alkaloids. *Chem. Sci.* **2021**, *12*, 4132. [[CrossRef](#)]
8. Guo, C.J.; Yeh, H.H.; Chiang, Y.M.; Sanchez, J.F.; Chang, S.L.; Bruno, K.S.; Wang, C.C.C. Biosynthetic Pathway for the Epipolythiodioxopiperazine Acetylaranotin in *Aspergillus terreus* Revealed by Genome-Based Deletion Analysis. *J. Am. Chem. Soc.* **2013**, *135*, 7205–7213. [[CrossRef](#)] [[PubMed](#)]
9. Zhu, M.L.; Zhang, X.M.; Feng, H.M.; Dai, J.J.; Li, J.; Che, Q.; Gu, Q.Q.; Zhu, T.J.; Li, D.H. Penicisulfuranols A–F, Alkaloids from the Mangrove Endophytic Fungus *Penicillium janthinellum* HDN13-309. *J. Nat. Prod.* **2017**, *80*, 71–75. [[CrossRef](#)] [[PubMed](#)]
10. Meng, L.H.; Zhang, P.; Li, X.M.; Wang, B.G. Penicibrocazines A–E, Five New Sulfide Diketopiperazines from the Marine-Derived Endophytic Fungus *Penicillium brocae*. *Mar. Drugs* **2015**, *13*, 276–287. [[CrossRef](#)] [[PubMed](#)]
11. Xu, X.Y.; Tan, Y.H.; Gao, C.H.; Liu, K.; Tang, Z.Z.; Lu, C.J.; Li, H.Y.; Zhang, X.Y.; Liu, Y.H. New 3-Acyl Tetramic Acid Derivatives from the Deep-Sea-Derived Fungus *Lecanicillium fusisporum*. *Mar. Drugs* **2022**, *20*, 255. [[CrossRef](#)]
12. Poolsawas, S.; Napisintuwong, O. Speed of hybrid maize adoption in Thailand: An application of duration analysis. *J. ISSAAS* **2019**, *25*, 95–103.
13. Su, L.; Zhu, H.; Guo, Y.X.; Du, X.P.; Guo, J.G.; Zhang, L.; Qin, C. *Lecanicillium coprophilum* (Cordycipitaceae, Hypocreales), a new species of fungus from the feces of *Marmota monax* in China. *Phytotaxa* **2019**, *387*, 055–062. [[CrossRef](#)]
14. Ishidoh, K.I.; Kinoshita, H.; Igarashi, Y.; Ihara, F.; Nihira, T. Cyclic lipodepsipeptides verlamelin A and B, isolated from entomopathogenic fungus *Lecanicillium* sp. *J. Antibiot.* **2014**, *67*, 459–463. [[CrossRef](#)] [[PubMed](#)]
15. Wang, Z.Y.; Sang, X.N.; Sun, K.; Huang, S.D.; Chen, S.S.; Xue, C.M.; Ban, L.F.; Li, Z.L.; Hua, H.M.; Peia, Y.H.; et al. Lecanicillones A–C, three dimeric isomers of spiciferone A with a cyclobutane ring from an entomopathogenic fungus *Lecanicillium* sp. PR-M-3. *RSC Adv.* **2016**, *6*, 82348. [[CrossRef](#)]
16. Wang, Z.Y.; Chen, S.S.; Sang, X.N.; Pan, H.Q.; Li, Z.L.; Hua, H.M.; Han, A.H.; Bai, J. Lecanicillolide, an α -pyrone substituted spiciferone from the fungus *Lecanicillium* sp. PR-M-3. *Tetrahedron Lett.* **2017**, *58*, 740–743. [[CrossRef](#)]
17. Kawahara, N.; Nozawa, K.; Nakajim, S.; Yamazaki, M.; Kawai, K. Sulfur-containing Dioxopiperazine Derivatives from *Emericella heterothallica*. *Heterocycles* **1989**, *29*, 397–402.
18. Wang, L.S.; Zong, S.K.; Wu, P.P.; Sun, X.L.; Wu, C.Z.; Wang, H.T.; Zhu, M.L. Two new alkaloids produced by *Dothideomycetes* sp. BMC-101 isolated from the *Magnolia grandiflora*. *J. Asian Nat. Prod. Res.* **2022**, *25*, 731–740. [[CrossRef](#)]
19. Haritakun, R.; Rachtawee, P.; Komwijit, S.; Nithithanasilp, S.; Isaka, M. Highly Conjugated Ergostane-Type Steroids and Aranotin-Type Diketopiperazines from the Fungus *Aspergillus terreus* BCC 4651. *Helv. Chim. Acta* **2012**, *95*, 308–313. [[CrossRef](#)]
20. He, T.; Wang, Y.D.; Du, L.Q.; Li, F.G.; Hu, Q.F.; Cheng, G.G.; Wang, W.G. Overexpression of Global Regulator LaeA Induced Secondary Metabolite Production in *Aspergillus versicolor* 0312. *Rec. Nat. Prod.* **2020**, *14*, 387–394. [[CrossRef](#)]
21. Neuss, N.; Nagarajan, R.; Molloy, B.B.; Huckstep, L.L. Aranotin and related metabolites. II. Isolation, characterization, and structures of two new metabolites. *Tetrahedron Lett.* **1968**, *9*, 4467–4471. [[CrossRef](#)]
22. Li, Y.; Yue, Q.; Krausert, N.M.; An, Z.Q.; Gloer, J.B.; Bills, G.F. Emestrins: Anti-Cryptococcus Epipolythiodioxopiperazines from *Podospora australis*. *J. Nat. Prod.* **2016**, *79*, 2357–2363. [[CrossRef](#)] [[PubMed](#)]
23. Yurchenko, A.N.; Berdyshev, D.V.; Smetanina, O.F.; Ivanets, E.V.; Zhuravleva, O.I.; Rasin, A.B.; Khudyakova, Y.V.; Popov, R.S.; Dyshlovoy, S.A.; Amsberg, G.V.; et al. Citriperazines A–D produced by a marine algaederived fungus *Penicillium* sp. KMM 4672. *Nat. Prod. Res.* **2020**, *34*, 1118–1123. [[CrossRef](#)] [[PubMed](#)]
24. Wu, J.S.; Shi, X.H.; Yao, G.S.; Shao, C.L.; Fu, X.M.; Zhang, X.L.; Guan, H.S.; Wang, C.Y. New Thiodiketopiperazine and 3,4-Dihydroisocoumarin Derivatives from the Marine-Derived Fungus *Aspergillus terreus*. *Mar. Drugs* **2020**, *18*, 132. [[CrossRef](#)]
25. Cai, C.L.; Waring, P. Redox sensitive epidithiodioxopiperazines in biological mechanisms of toxicity. *Redox Rep.* **2000**, *5*, 257–264.
26. Orfali, R.S.; Aly, A.H.; Ebrahim, W.; Abdel-Aziz, M.S.; Muller, W.E.G.; Lin, W.H.; Daletos, G.; Proksch, P. Pretrichodermamide C and N-methylpretrichodermamide B, two new cytotoxic epidithiodiketopiperazines from hyper saline lake derived *Penicillium* sp. *Phytochem. Lett.* **2015**, *11*, 168–172. [[CrossRef](#)]
27. Liang, X.; Huang, Z.H.; Ma, X.; Zheng, Z.H.; Zhang, X.X.; Lu, X.H.; Qi, S.H. Mycotoxins as inhibitors of protein tyrosine phosphatases from the deep-sea-derived fungus *Aspergillus puniceus* SCSIO z021. *Bioorganic Chem.* **2021**, *107*, 104571. [[CrossRef](#)]

28. Liu, C.M.; Yao, F.H.; Lu, X.H.; Zhang, X.X.; Luo, L.X.; Liang, X.; Qi, S.H. Isoquinoline Alkaloids as Protein Tyrosine Phosphatase Inhibitors from a Deep-Sea-Derived Fungus *Aspergillus puniceus*. *Mar. Drugs* **2022**, *20*, 78. [[CrossRef](#)]
29. Wang, J.; Nong, X.H.; Amin, M.; Qi, S.H. Hygrocin C from marine-derived *Streptomyces* sp. SCSGAA 0027 inhibits biofilm formation in *Bacillus amyloliquefaciens* SCSGAB0082 isolated from South China Sea gorgonian. *Appl. Microbiol. Biotechnol.* **2018**, *102*, 1417–1427. [[CrossRef](#)]

Disclaimer/Publisher’s Note: The statements, opinions and data contained in all publications are solely those of the individual author(s) and contributor(s) and not of MDPI and/or the editor(s). MDPI and/or the editor(s) disclaim responsibility for any injury to people or property resulting from any ideas, methods, instructions or products referred to in the content.